



المملكة العربية السعودية  
وزارة التعليم  
جامعة الإمام محمد بن سعود الإسلامية  
كلية العلوم  
قسم الفيزياء

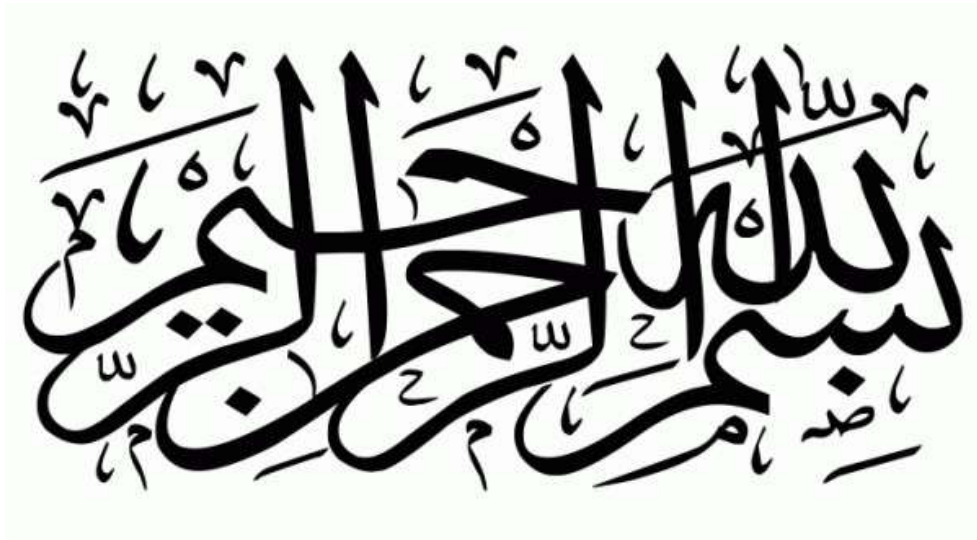
## **H<sub>2</sub>S gas sensor based on NiFe<sub>2</sub>O<sub>4</sub> nanoparticles**

by

**Abdulaziz bin abdurhman AL-mousa**

**Supervised by:**

**Dr. Mokhtar Hjiri**



## ABSTRACT

Nickel ferrite ( $\text{NiFe}_2\text{O}_4$ ) nanopowders were synthesized by hydrothermal technique. The obtained powders are characterized by means of X-ray diffraction (XRD). The prepared nanopowders exhibited cubic structure. The average crystallites size is 10 nm.  $\text{H}_2\text{S}$  sensing tests were done using different gas concentrations (from 0.125 to 5 ppm). The fabricated gas sensors exhibited high sensitivity of 90 toward low  $\text{H}_2\text{S}$  concentrations of 5 ppm. Using a mixture of gases, the fabricated sensor showed that it was selective to  $\text{H}_2\text{S}$  gas. Results demonstrated that  $\text{NiFe}_2\text{O}_4$  might be promising sensing materials for the detection of  $\text{H}_2\text{S}$  at low operating temperature.

## المستخلص

تم تصنيع مساحيق نانوية من فيريت النيكل بتقنية الهيدروحرارية. تتميز المساحيق الناتجة عن طريق حيود الأشعة السينية. أظهرت مساحيق النانو المحضرة بنية مكعبة. يبلغ متوسط حجم البلورات 10 نانومتر. تم إجراء اختبارات استشعار كبريتيد الهيدروجين باستخدام تركيزات غازية مختلفة (من 0.125 إلى 5 جزء في المليون). أظهر مستشعر الغاز المصنوع حساسية عالية تبلغ 90 تجاه تركيز كبريتيد الهيدروجين المنخفض البالغ 5 جزء في المليون. باستخدام مزيج من الغازات، أظهر المستشعر المصنوع أنه انتقائي لغاز كبريتيد الهيدروجين. أخيرًا، أظهرت النتائج أن فيريت النيكل قد يكون مواد استشعار واعدة للكشف عن كبريتيد الهيدروجين عند درجة حرارة تشغيل منخفضة.

# Table of contents

General Introduction .....	3
<b>Chapter 1: overview on gas sensors</b> .....	4
1.1. Introduction .....	5
1.2. Gas sensors definition .....	5
1.3. Gas sensors structure.....	7
1.4. Metal oxides semiconductors gas sensors.....	8
1.5. Gas sensors principle .....	8
1.6. Gas sensing properties .....	11
1.6.1. Sensitivity .....	11
1.6.2. Stability .....	11
1.6.3. Selectivity .....	12
1.6.4. Working temperature .....	12
1.6.5. Response and recovery time .....	12
1.7. Conclusion .....	13
<b>Chapter 2: experimental details</b> .....	14
2.1. Introduction.....	15
2.2. ZnO and Mg-doped ZnO nanopowders synthesis .....	15
2.3. X-ray diffraction measurement .....	16
2.4. Gas sensors tests .....	17

2.4.1. Gas sensors fabrication .....	17
2.4.2. Gas sensors testing .....	19
2.5. Conclusion .....	21
<b>Chapter 3: results and discussion</b> .....	<b>22</b>
3.1. Introduction .....	23
3.2. Structural properties of pure ZnO and Mg-doped ZnO nanoparticles .....	23
3.3. NO <sub>2</sub> gas sensors tests .....	26
3.3.1. NO <sub>2</sub> gas sensors based on ZnO nanoparticles .....	27
3.3.2. NO <sub>2</sub> gas sensors based on Mg-doped ZnO nanoparticles .....	29
3.4. Conclusion .....	35
General conclusion .....	

## General introduction

Hydrogen sulfide is colorless, flammable and very toxic gas used in laboratories as well at several industries. It can be produced from organic compounds decomposition, like waste of animals. The danger of  $\text{H}_2\text{S}$  gas is that it leads to the irritation of eyes, respiration difficulties, respiratory effects to asthmatic patients, in addition to cough when exposed to low concentrations [1]. The development of efficient  $\text{H}_2\text{S}$  sensor is then of great interest in the environmental control and monitoring.

In this report, we studied the structural properties of nickel ferrite and its gas sensing properties such as gas response, operating temperature, selectivity, response time and recovery time.

This report is composed of three parts:

**Chapter one:** gives a generality about gas sensors.

**Chapter two:** presents the protocol for  $\text{NiFe}_2\text{O}_4$  powders synthesis, X-ray diffraction (XRD) technique and it describes the gas sensing device.

**Chapter three:** illustrates all the obtained results and the discussion.

# **Chapter 1: Generality on Gas Sensors**

## **1.1. Introduction**

Gas sensing is a critical technology that detects various gases in the environment. Gas sensors are devices designed to respond to specific types of gases. In this chapter, an overview on gas sensors has been suggested.

## **1.2. Gas sensors definition**

A gas sensor is a device that converts chemical quantity into typically electrical signal. Generally it is composed of two main parts: the sensing element and transducer. The sensing element is the heart of the sensor on which the reaction happens with the gaseous species and the transducer is the device transforming the result of the interaction in an easily readable in most cases an electrical signal.



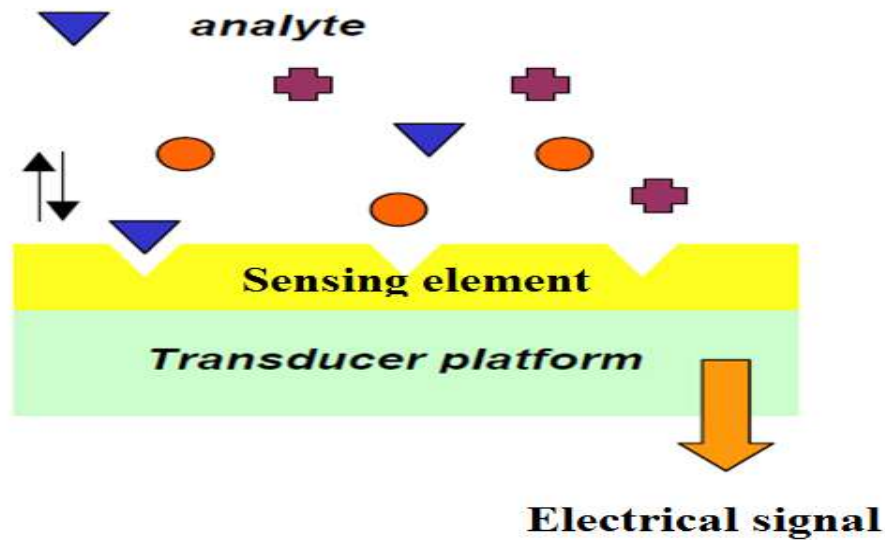


Figure 1.1. Gas sensor device

Metal oxide semiconductors gas sensors were introduced for the first time in the practical use by Taguchi at the beginning of the 70' years. They are used as:

- ❖ Alarms to prevent accidents in domestic houses,
- ❖ Humidity sensors in the alimentary,
- ❖ Sensors in the automotive sector,
- ❖ Breath analyzers for medical diagnosis.

### 1.3. Gas sensors structure

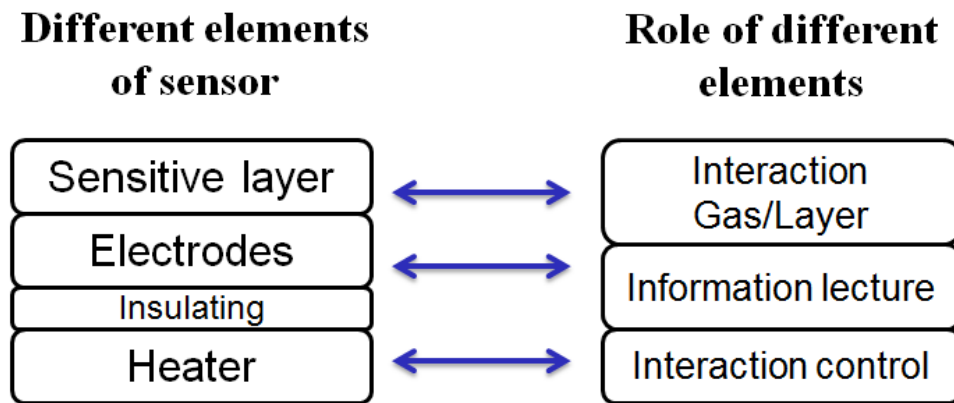


Figure 1.2. Gas sensor components

Gas sensors are composed of:

- A sensitive layer, constituting the part that will interact with the gaseous molecules.
- Electrodes for electrical measurement of the sensitive layer.
- A heating part to bring the temperature-sensitive layer.
- Insulator that isolates electrodes from heater.

#### 1.4. Metal oxides Semiconductors gas sensors

The metal oxides semiconductors gas sensors belong to electric gas sensors family. This type depends on the electric properties measurements (in our case the measurement of electric resistance).

Besides, the resistance of this type of gas sensors was strongly affected

by the interaction between gas molecules and the semiconductor material.

Among these materials, we can cite: ZnO, CuO, SnO<sub>2</sub>, TiO<sub>2</sub>, WO<sub>3</sub>, Fe<sub>2</sub>O<sub>3</sub>...etc.

### **1.5. Gas sensor principle**

The basic principle of detection is the result of the interaction between a sensitive material and the surrounding gas, which is accompanied by a change in the physicochemical properties of the material. By a process of transducing an electrical signal, optical, mechanical or thermal will be generated. These variations are related to the nature, concentration of gas in interaction and measurement conditions.

For metal oxide semiconductors based gas sensors, In first approximation, oxygen adsorbed on the surface of n-type metal oxide semiconductors plays a key role, trapping free electrons because of its high electron affinity, and forming a potential barrier at the grain boundaries. This potential barrier restricts the flow of electrons, causing the electric resistance to increase (Figure 2.3).

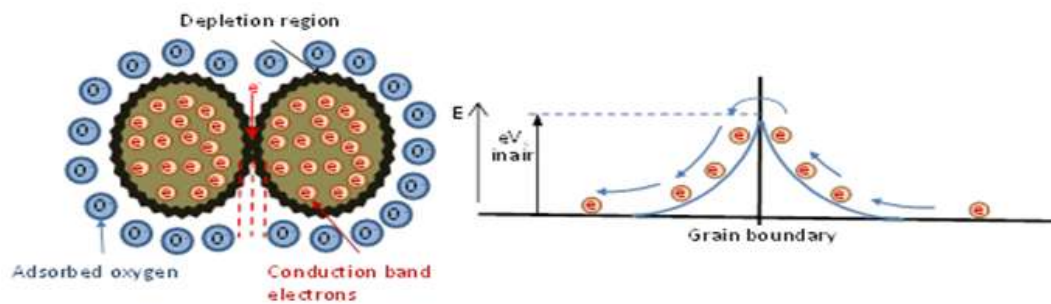


Figure 1.3. Oxygen molecules interaction with sensing layer.

When the gas sensor was exposed to reducing gases such as carbon monoxide (CO), the gas molecules are adsorbed on the sensing layer surface and reacted with active oxygen species, which liberated free electrons.

This lowered the potential barrier allowing electrons to flow more easily, then reducing the electric resistance (Figure 1.4).

With oxidizing gases such as  $\text{NO}_2$ , the adsorption process increased instead the electric resistance.

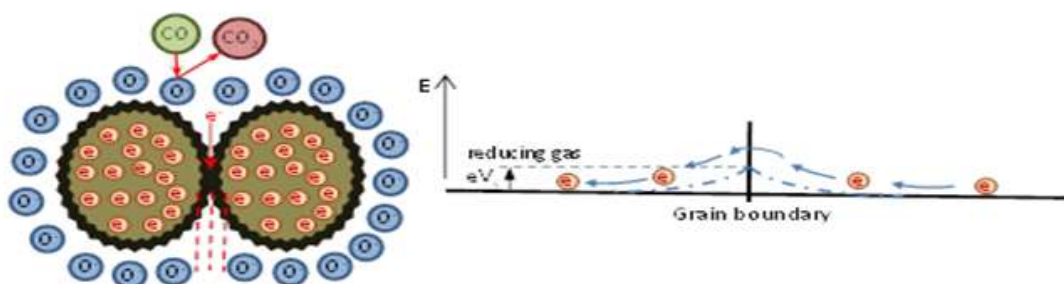


Figure 1.4. Interaction of gas molecules with adsorbed oxygen species.

## **1.6. Gas sensing properties**

### *1.6.1. Sensitivity*

The sensitivity (S) was a measure of the extent of change in material resistance when exposed to target gas. As example, for oxidizing gas such as NO<sub>2</sub>, the sensitivity is presented by the following expressions:

$$S = \frac{R_{\text{gas}}}{R_{\text{air}}} \quad \text{for n-type semiconductor}$$

$$S = \frac{R_{\text{air}}}{R_{\text{gas}}} \quad \text{for p-type semiconductor}$$

### *1.6.2. Stability*

It is defined as the ability of the gas sensor to perform a consistent measurement for a specific time period at various gas concentrations. This implies the ability of the sensor to retain the same performances in terms of sensitivity, selectivity, response, and recovery time.

### *1.6.3. Selectivity*

Selectivity is the ability of the sensor to detect single target gas when it is exposed to a mixture of gases.

#### *1.6.4. Working temperature*

The temperature that corresponds to the higher sensitivity is called the working temperature. This parameter is essential for the gas sensing operation.

#### *1.6.5. Response and recovery times*

The **response time** is defined as the time needed for the sensor response to arrive at 90 % of its maximum when exposed to target gas. With the elimination of gas exposure, there is a time to return to its equilibrium state; in this case we speak about **recovery time** (Figure 1.5).

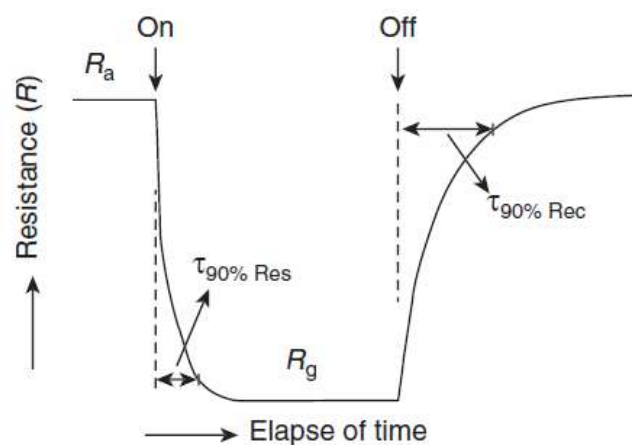


Figure 1.5. Response/recovery times

## **1.7. Conclusion**

In this chapter, we have introduced an overview on chemical gas sensor and their performances. Among the chemical gas sensors metal oxide semiconductors (MOS) gas sensors are largely used because they are small and have good yield and low cost.

## Chapter 2: experiment details



## **2.1. Introduction**

In this chapter, we presented the protocol of synthesis of  $\text{NiFe}_2\text{O}_4$  nanopowders using hydrothermal technique. A brief description of X-ray diffraction technique was suggested. In addition to a presentation of the sensing tests device made at the University of Messina, Italy.

## **2.2. Synthesis of nickel ferrite nanopowders**

The hydrothermal technique was utilized to synthesize spinel nickel ferrite nanoparticles with nickel concentration of 25 at.%. The starting materials were  $\text{NiCl}_2$  as salt of nickel and  $\text{FeCl}_3$  as salt of iron. These two precursors were dissolved in distilled water after magnetic stirring. Then, 2 ml of ammonia were added to the solution. The final solution was poured into Teflon lined steel autoclave which was kept for heating in programmed furnace at 200 °C for 6 h. The resultant materials are washed several times with mixture of ethanol and water for purification and then dried at 60 °C for 1 h in an oven. A heat treatment at 500 °C for 2 hours is necessary for the crystallization of the obtained powders.

## **2.3. X-ray diffraction measurement**

X-ray diffraction is a non-destructive technique with which it is possible to obtain information about the crystalline phase composition of a

sample, along with other structural information such as lattice parameters, strain, and grain size.

It is based on constructive interference of monochromatic X-rays and a crystalline sample. The interaction of the incident rays with the sample produces constructive interference when conditions satisfy Bragg's law (2.1). This law relates the wavelength electromagnetic radiation to the diffraction angle and the lattice spacing in a crystalline sample.

$$n\lambda = 2d \cdot \sin\theta \quad 2.1$$

The microstructure of the samples in this thesis was investigated by XRD (Bruker AXS D8 Advance) using the CuK $\alpha$ 1 wavelength of 1.5405 Å. The average crystallite size was calculated using the Scherer's formula [2]:

$$D = \frac{K\lambda}{\beta \cos \theta} \quad 2.2$$

where K is a dimensionless shape factor, with a value close to unity (the shape factor has a typical value of about 0.9),  $\lambda$  is the X-ray wavelength,  $\beta$  is the full width at half maximum (FWHM) of the XRD peak.

## 2.4. Gas sensing tests

### 2.4.1. Gas sensor fabrication

For gas testing gas sensors, it is necessary to fabricate gas sensor elements. The element is composed of a sensing material; interdigitated electrodes and heater (Figure 2.1). The sensing materials are semiconducting metal oxides. The electrodes and the heater are on platinum and the substrate is on alumina. The platinum and the alumina are used because of their high thermal stability. The active sensing layer was deposited on the Pt interdigitated electrodes area from an aqueous paste of the samples by screen printing.

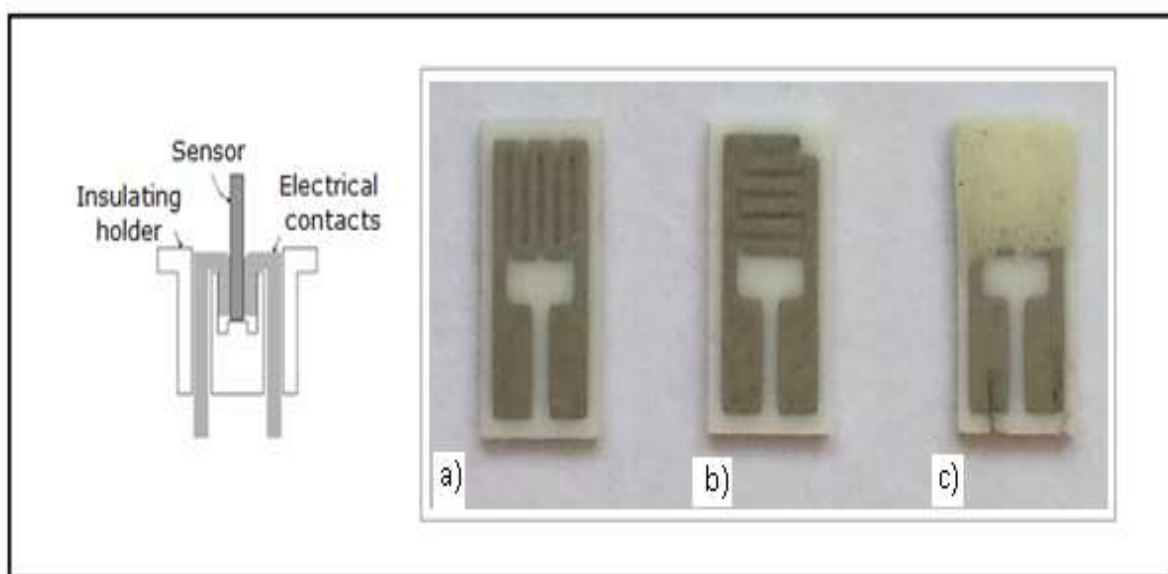


Figure 2.1. Sensor device and its structure. a) Pt heater; b) Pt interdigitated electrodes; c) printed film.

### 2.4.2. Gas sensor testing

The fabricated sensor was introduced in a stainless-steel test chamber (Figure 2.2) for the sensing tests. In general the sensing mechanism is affected by the operating temperature. Therefore, the response of the fabricated sensor as a function of the operating temperature was first investigated.

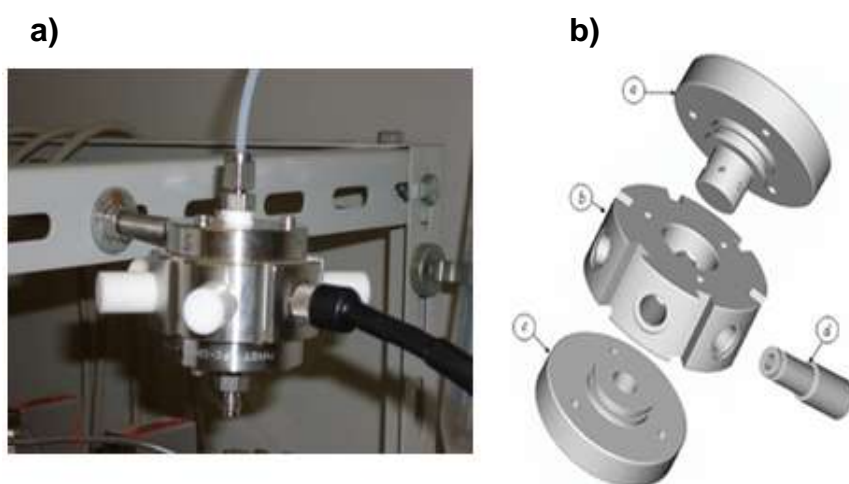


Figure 2.2. Photograph (a) and scheme (b) of the stainless-steel test chamber.

Gases coming from certified bottles can be further diluted in air at a given concentration by mass flow controllers (Figure 2.3). Electrical measurements were carried out in the temperature range from 50 to 400

°C, with steps of 50 °C, under a dry air, collecting the sensors resistance data in the four point mode.



Figure 2.3. Mass flow controllers.

## 2.5. Conclusion

In this chapter we described the protocol of synthesis of  $\text{NiFe}_2\text{O}_4$  mentioned in this report. To show the structure of these samples, X-ray diffraction analysis was performed. For sensing tests, we have tested our sample by an apparatus installed in the Italian laboratory.

## Chapter 3: Results and discussion

### 3.1. Introduction

In this chapter, we discussed the obtained results from XRD analyses and  $\text{H}_2\text{S}$  gas sensing tests.

### 3.2. Structural properties of $\text{NiFe}_2\text{O}_4$ nanoparticles

X-ray powder diffraction analysis was carried out to investigate the crystal structures of  $\text{NiFe}_2\text{O}_4$  sample. Figure 3.1 showed the X-ray diffraction spectrum of  $\text{NiFe}_2\text{O}_4$  nanopowders.

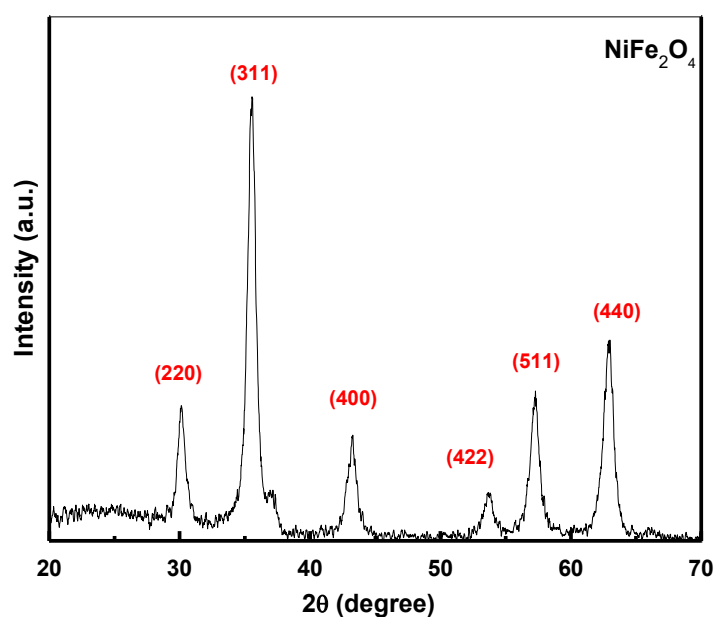


Figure 3.1. X-ray diffraction spectrum of  $\text{NiFe}_2\text{O}_4$  nanopowders.

Nickel ferrite nanopowder presented diffraction peaks at  $2\theta = 30.2^\circ$ ,  $35.4^\circ$ ,  $37.13^\circ$ ,  $43.21^\circ$ ,  $53.63^\circ$ ,  $57.11^\circ$ ,  $62.71^\circ$ , correspond to the spinel phase (JCPDS N°01-074-2081). The previous peaks indicated that  $\text{NiFe}_2\text{O}_4$  exhibited cubic structure.

Table 3.1. Structural parameters of pure ZnO nanopowders

Planes	Angle $2\theta$ ( $^\circ$ )	$\beta$ ( $^\circ$ )	$\beta$ (radian)	D (nm)
(220)	30.12	0.58813	0.01026	14
(311)	35.64	0.70812	0.01236	11.78
(400)	43.36	0.8334	0.01454557	10
(422)	53.79	0.78608	0.01371968	11.05
(511)	57.33	0.75838	0.01323622	11.92
(440)	62.96	0.71752	0.01252308	12.98

The average crystallites size of  $\text{NiFe}_2\text{O}_4$  was  $D_{\text{avg}} = 11.96$  nm.

Table 3.1 presented the crystallites size for each diffraction peak, calculated using Scherer equation, for nickel ferrite nanopowders. As suggested by the table above, the average crystallites size is found to be 11.96 nm.



### 3.3. Hydrogen sulfide sensing tests

In this part, we studied the gas sensing properties of the  $\text{NiFe}_2\text{O}_4$  nanoparticles toward  $\text{H}_2\text{S}$  gas with different concentrations.

The  $\text{H}_2\text{S}$  gas concentrations used in this study were: 0.126, 0.315, 0.630, 1.26, 3.15 and 5.04 ppm.

The operating temperature selected to make sensing tests was  $T = 200^\circ\text{C}$ .

#### 3.3.1. $\text{H}_2\text{S}$ gas sensor based on $\text{NiFe}_2\text{O}_4$ nanoparticles

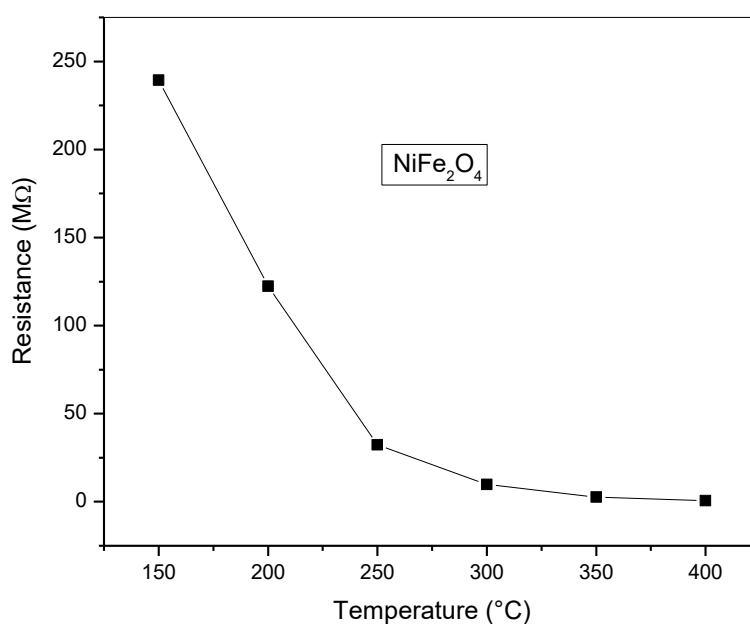


Figure 3.2. Variation of resistance versus working temperature of  $\text{NiFe}_2\text{O}_4$  material

The variation of nickel ferrite resistance as a function of the operating temperature was displayed in Figure 3.2. At low temperature ( $T = 150^\circ\text{C}$ ), the suggested sample exhibited higher electric resistance (about 230

M $\Omega$ ). Increasing the temperature yields to a decrease of the resistance indicating the semiconductor behavior of the material. This is due to the thermal excitation of electrons into the conduction band .

Since the working temperature was an important factor that influenced the sensitivity, the response-temperature variation of NiFe<sub>2</sub>O<sub>4</sub> sensor toward 1.3 ppm of H<sub>2</sub>S gas was suggested in Figure 3.3. At T = 150 °C, the fabricated sensor achieved a maximum value of 51. The maximum response indicated that the temperature was enough for the interaction between gas molecules and adsorbed oxygen species since the raise of thermal energy of gas molecules overcomes the activation energy barrier of the surface reaction with adsorbed oxygen anions [3]. Another reason for the higher sensitivity was the increase of free electrons number because of the adsorbed oxygen species conversion to O<sup>-</sup> [4]. With the increase of temperature the gas response began to decrease. This behavior might be attributed to gas adsorption ability reduction for the higher temperatures [5].

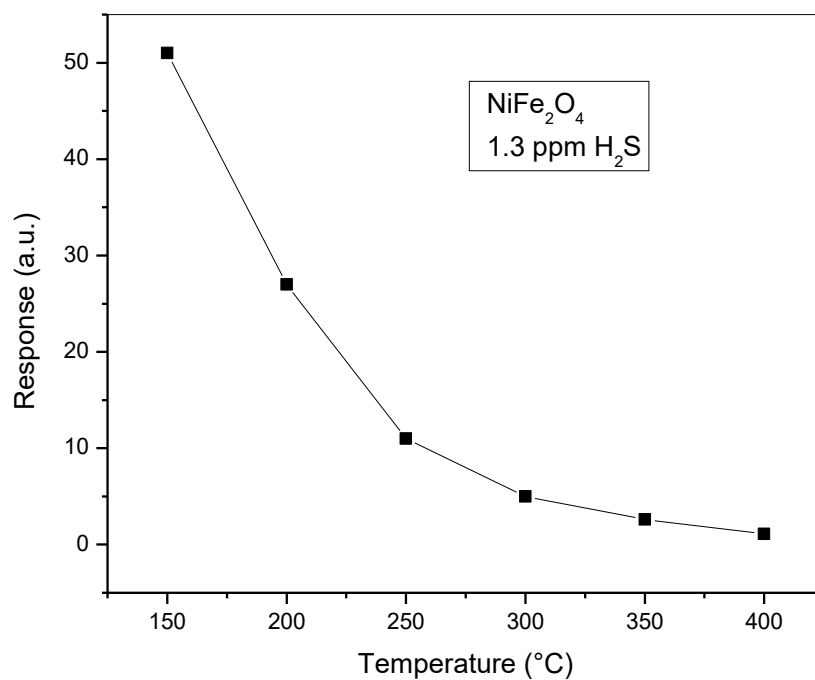


Figure 3.3. Variation of gas response toward 1.3 ppm of  $\text{H}_2\text{S}$  versus working temperature

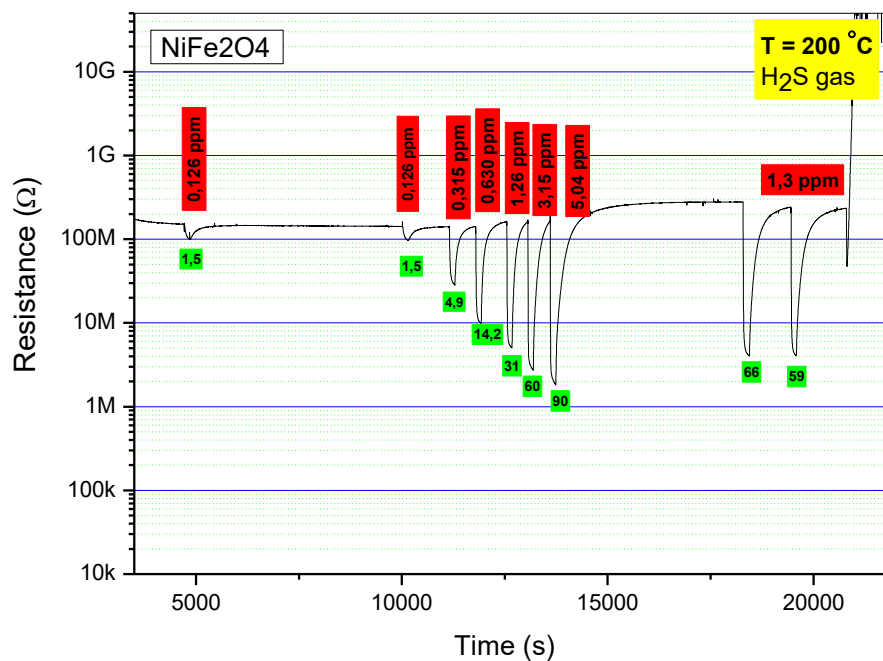


Figure 3.4. Resistance-gas concentration dependence of  $\text{NiFe}_2\text{O}_4$  sensor at  $200^{\circ}\text{C}$

It was clearly seen in Figure 3.4 that the fabricated sensor was sensitive to the target gas even at low gas concentrations ( $S = 1.5$  toward 0.126 ppm). Furthermore, an increase in  $H_2S$  concentration from 0.126 to 5.04 ppm yields to more decrease in the material electric resistance. Since  $H_2S$  is considered as a reducing gas, it then resulted from its interaction with adsorbed oxygen species a loss of electrons leading to conductivity increase and a resistance decrease of the sensing layer, indicating the n-type behavior of the suggested material. The resistances had good reversibility during the exposure and exhaust cycles of  $H_2S$  gas.

The response and recovery times are considered important parameters to say that the sensor is good and efficient. The response and recovery are found to be 10 and 170 s, respectively. Ghosh et al. obtained response and recovery times of 90 and 300 s when the  $NiFe_2O_4$  sensor is exposed to 200 ppm of  $H_2S$  [6].

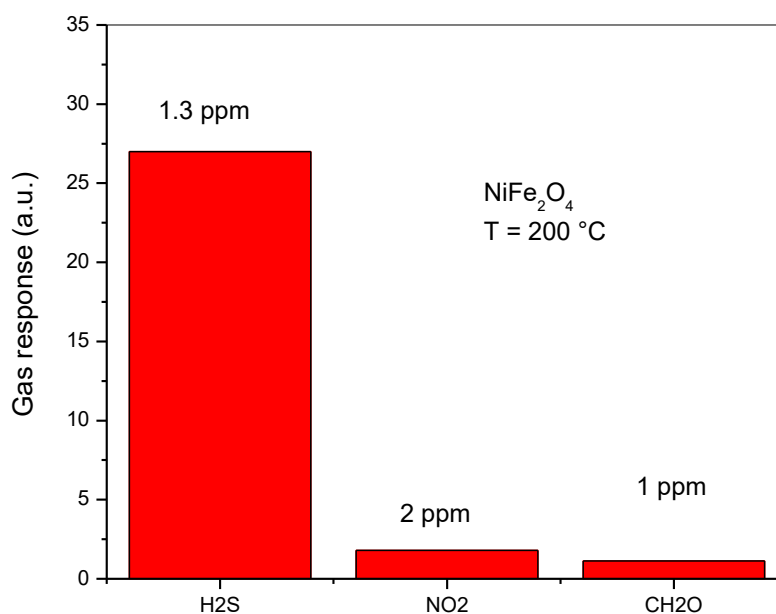


Figure 3.5. Response of NiFe<sub>2</sub>O<sub>4</sub> sensor toward different gases

To show the selectivity of the suggested sensor, NiFe<sub>2</sub>O<sub>4</sub> was tested toward several gases such as NO<sub>2</sub>, CH<sub>2</sub>O and H<sub>2</sub>S. As seen, our sensor exhibited the highest response toward H<sub>2</sub>S gas compared to other gases.

### 3.4. Conclusion

In this chapter, nickel ferrite nanopowders were prepared by hydrothermal technique. The sensor exhibited a good response toward H<sub>2</sub>S gas at T = 200 °C. The fabricated sensor was selective to this gas when exposed to various gases.

## References

- [1] I.P.o.C.S.a.W.H. Organisation, Concise International Chemical Assessment, Document 53 – Hydrogen Sulphide: Human Health Aspects World Health Organization Geneva, Switzerland, 2003
- [2] H. Saeki, H. Tabata, T. Kawai, Solid State Commun. 120 (2001) 439
- [3] G. Zhang, C. Li, F. Cheng, J. Chen, Sensors and Actuators B: Chemical 120 (2007) 403–410
- [4] J. Zhang, J.M. Song, H.L. Niu, C.J. Mao, S.Y. Zhang, Y.H. Shen, Sens Actuators B Chem 221 (2015) 55
- [5] G. Zhang, C. Li, F. Cheng, J. Chen, Sensors and Actuators B: Chemical 120 (2007) 403–410
- [6] P. Ghosh, A. Mukherjee, M. Fu, S. Chattopadhyay, P. Mitra, Physica E: Low-dimensional Systems and Nanostructures 74 (2015) 570-575